-RESEARCH PAPER-

International Journal of Mining and Geo-Engineering

IJMGE

IJMGE 60-1 (2026) 1-7

DOI: 10.22059/IJMGE.2026.399561.595284

Fracture mechanisms in rock-like Bi-material beams under mode I loading: effects of crack location and thickness ratio

Ehsan Ghavimi [a], Mosleh Eftekhari [a, *] and Hamid Reza Nejati [a]

[a] *Department of Mining Engineering, Faculty of Mining and Materials, Tarbiat Modares University, Tehran, Iran.*

Article History:

Received: 28 July 2025.

Revised: 07 September 2025.

Accepted: 02 March 2026.

ABSTRACT

Understanding the fracture behavior of bi-material systems is crucial in rock mechanics where material heterogeneity and interfacial discontinuities can significantly affect crack propagation. This study experimentally investigated the crack propagation mechanisms in layered specimens composed of two cementitious materials with deliberately contrasting mechanical properties. Six bi-material configurations were tested under three-point bending using pre-notched beams, with variations in layer thickness and initial notch location. Single-material tests were also conducted to determine the uniaxial compressive strength, tensile strength, and fracture toughness of each constituent material. The results demonstrated that notch location and relative layer thickness significantly influenced fracture behavior. Cracks originating in the stiffer material typically propagated directly across the interface. In contrast, cracks initiated in the weaker material often showed deflection or staged propagation. Load–displacement curves reflected these differences, with specimens containing notches in the weaker material exhibiting lower peak loads, and in some cases, multiple load peaks. The experimental findings contribute to a deeper understanding of interface-controlled fracture behavior in rock-like composites and provide valuable data for validating future numerical simulations.

Keywords: *Bi-material interface, Rock-like material, Crack propagation, Three-point bending, Fracture toughness.*

1. Introduction

In many underground and civil engineering applications, bi-material systems formed by bonding two cementitious or rock-like layers are widely used. Examples include rock–shotcrete linings, grout-injected rock joints, and concrete–rock interfaces in tunnel support systems [1-3]. In such configurations, an interface with contrasting mechanical properties plays a decisive role in determining the fracture response of the system [1, 4]. Depending on the relative stiffness, tensile strength, and fracture energy of the adjacent materials, this interface may act either as a crack path of weakness or as a barrier to crack penetration [4, 5].

Crack propagation near interfaces has been studied extensively, especially in metallic and polymeric composites [6-9]. However, in rock-like and quasi-brittle materials, the mechanisms governing crack interaction with an interface—particularly for cracks approaching the interface perpendicularly—remain less understood. While many prior studies focus on interface-parallel or inclined cracks, fewer have examined the full evolution of cracks that cross the interface, especially under Mode I loading conditions [10, 11].

In this context, investigations on rock masses provide complementary insights into fracture mechanisms, since natural discontinuities such as joints and bedding planes can act as interfaces that strongly influence crack initiation and coalescence. For example, non-persistent joint geometries and environmental processes (e.g., freeze–thaw) have been shown to alter crack growth patterns and acoustic emission activity in brittle rocks [12]. Advanced synthetic and numerical approaches, including lattice-spring synthetic rock mass simulations, have further highlighted the role of joint distribution and non-persistence in controlling fracture trajectories and shear response [13]. Similarly, laboratory-scale studies emphasize that microstructural features such as grain size and texture significantly affect Mode I fracture toughness and crack propagation under tensile or flexural loading [14].

Theoretically, the singularity behavior at the tip of a crack near a bi-material interface has been well established. Zak and Williams [10] showed that the stress field at the crack tip exhibits an oscillatory singularity that depends on the elastic mismatch between materials. Cook and Erdogan [5] later derived exact stress intensity factors for cracks normal to an interface. For quasi-brittle media like mortar and rock, the fracture process zone (FPZ) introduces additional complexity, which has been modeled effectively using the fictitious crack model proposed by Hillerborg et al. [15] and applied in subsequent studies [16-21].

Recent researches have investigated crack behavior in rock–concrete and mortar–rock systems under various loading and environmental conditions, including interface roughness [1, 2, 22, 23], loading rate [24], and temperature or chemical exposure [25, 26]. Findings showed that when a crack propagates from a weaker material to a stronger one, an abrupt load increase may occur due to interface resistance [6, 15], whereas cracks moving in the opposite direction often experience smooth transition and rapid penetration [4, 27].

Despite these advances, experimental studies that specifically examine perpendicular crack penetration in layered rock-like composites under controlled flexural loading remain limited. Understanding how cracks behave in such settings is essential, especially since variations in layer thickness or interface strength may lead to

* Corresponding author. *Tel:* +98 21 82885016, *E-mail address:* : mosleh.eftekhari@modares.ac.ir (M. Eftekhari).

multiple load peaks or complex failure modes [4, 28]. Numerical and synthetic-rock studies suggest strong sensitivity to joint arrangement and material contrast [13], and recent predictive-modeling efforts for Mode I fracture toughness and crack initiation criteria motivate carefully controlled laboratory data for validation purposes [29-31].

To address this gap, the present study conducts Mode I fracture experiments on synthetic two-layer beams made from materials with contrasting mechanical properties. One material consists of a cement–water mixture, while the other combines cement and gypsum. pre-existing notches oriented normal to the horizontal interface are introduced, and the effect of notch location and thickness ratio on fracture behavior is investigated through three-point bending tests. This work aims to provide a deeper understanding of interface-controlled fracture mechanisms in bi-material quasi-brittle structures and to supply experimental data for validating future numerical models such as XFEM and lattice-based simulations [32-36]. The results have direct relevance for the design of safer underground structures involving layered or bonded cementitious materials.

2. Experimental program

2.1. Materials and mixture design

To create synthetic rock-like specimens with controlled and contrasting mechanical properties, two distinct cementitious mixtures were developed. Material 1 was prepared by mixing Portland cement and water at a water-to-cement ratio of 0.5, producing a stiff and high-strength material. Material 2 was formulated by blending gypsum, cement, and water at a mass ratio of 25%:37.5%:37.5%, resulting in a weaker, more compliant composite. These compositions were selected through preliminary trials to ensure a significant contrast in compressive strength and fracture toughness, necessary for evaluating crack-interface interactions.

2.2. Specimen preparation

Two types of specimens were prepared, both with identical overall dimensions: 320 mm in length (L), 80 mm in height (H), and 40 mm in thickness (T). A single edge notch (a), 15 mm in length, was introduced at mid-span on one side of each specimen, oriented perpendicular to the interface.

• **Single-material beams** were cast entirely from either Material 1 or Material 2, and used to determine mechanical properties including uniaxial compressive strength (UCS), Brazilian tensile strength (BTS), and Mode I fracture toughness via notched three-point bending tests.

• **Bi-material beams** were constructed by horizontally layering the two materials within the same overall geometry. The total height (80 mm) was divided between the two layers with thickness combinations of 30/50 mm, 40/40 mm, and 50/30 mm. In different configurations, either material could occupy the top or bottom layer, and the initial notch was placed in either material to evaluate the role of crack initiation side. This design enabled systematic investigation of how relative material thickness and crack origin affect fracture behavior, while keeping the external dimensions of the specimens consistent.

To ensure a clean and controlled interface, the first material was poured into a steel mold with a thin galvanized sheet acting as a separator. After initial setting, the sheet was carefully removed and the second material was cast on top. All specimens were demolded after 24 hours and cured in water for 28 days. Figure 1(a) presents a schematic illustration of the bi-material specimen, including the layer arrangement, notch orientation, and the three-point bending test setup. Figure 1(b) shows an experimental view of a specimen under three-point bending, offering a clear representation of the specimen configuration and loading conditions.

2.3. Pre-cracking and notch configuration

A vertical notch (15 mm long) was cut at the mid-span, oriented perpendicular to the horizontal interface, to simulate an initial crack. In different configurations, the notch was placed either in Material 1 or Material 2, allowing investigation of how crack initiation site and propagation direction influence interface interaction. Six configurations were tested, as summarized in Table 1.

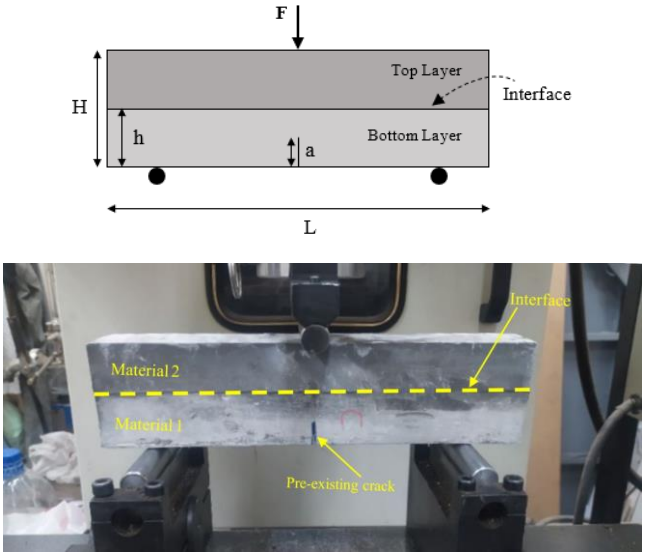

Figure 1. (a) Schematic illustration of the bi-material specimen, including layer configuration, notch orientation, and the three-point bending test setup (b) Experimental view of a bi-material specimen during a three-point bending test.

2.4. Mechanical testing

To characterize the mechanical behavior of the materials used in this study, a series of standardized mechanical tests were conducted on single-material specimens. All procedures were performed in accordance with relevant international standards to ensure consistency and repeatability. The mechanical parameters evaluated included uniaxial compressive strength (UCS), Brazilian tensile strength (BTS), and Mode I fracture toughness. These tests provided a reference for assessing the mechanical contrast between the two materials and allowed quantification of their elastic properties, strength, and fracture energy characteristics.

Fracture tests on bi-material beams were carried out under a three-point bending configuration using pre-notched specimens. The span between the supports was 240 mm, and the load was applied at the mid-span through a steel loading roller. The experiments were performed using a universal testing machine, and the applied load and corresponding displacement were continuously recorded. During each test, crack initiation, propagation path, and interactions with the material interface were carefully observed. In all specimens, the notch was oriented perpendicular to the interface. Various combinations of layer thicknesses and notch positions were considered to investigate the effects of geometry and material configuration on the fracture behavior. For each configuration (both single- and bi-material), two replicate specimens were tested to ensure the repeatability of results.

3. Results and discussion

3.1. Mechanical properties of single-material specimens

To provide a reliable basis for interpreting the fracture response of bi-material specimens, a series of mechanical tests was first carried out on specimens made from each material. The two cementitious mixtures used—referred to as Material 1 and Material 2—were intentionally formulated to have contrasting mechanical behavior. Material 1 was composed solely of cement and water, whereas Material 2 included a blend of cement, gypsum, and water. These formulations led to significant differences in their mechanical properties, as summarized in Table 2.

Table 1. Geometry and crack location of bi-material specimens.

Specimen code	Layer thickness (bottom/top)	Pre-notch Location	Description
E-M1	40 mm (M1) / 40 mm (M2)	Material 1	Equal thickness; notch in the stiffer material (M1)
E-M2	40 mm (M2) / 40 mm (M1)	Material 2	Equal thickness; notch in the weaker material (M2)
T1-M1	50 mm (M1) / 30 mm (M2)	Material 1	M1 thicker; notch in the stiffer material (M1)
T1-M2	30 mm (M2) / 50 mm (M1)	Material 2	M1 thicker; notch in the weaker material (M2)
T2-M1	30 mm (M1) / 50 mm (M2)	Material 1	M2 thicker; notch in the stiffer material (M1)
T2-M2	50 mm (M2) / 30 mm (M1)	Material 2	M2 thicker; notch in the weaker material (M2)

Table 2. Mechanical properties of single-material specimens.

Material type	Uniaxial compressive strength (MPa)	Elastic modulus (GPa)	Tensile strength (MPa)
Material 1	34.52	21.08	3.19
Material 2	18.63	7.69	1.82

Experimental results demonstrated that Material 1 exhibited notably higher compressive and tensile strengths compared to Material 2. The incorporation of gypsum in Material 2 reduced its overall mechanical strength and stiffness, making it a suitable counterpart for studying fracture behavior across interfaces with mechanical contrast.

To further assess the crack resistance of the materials, Mode I fracture toughness tests were conducted using pre-notched beams under three-point bending. The fracture toughness KIC was determined according to standard analytical expressions based on peak load and specimen geometry. The corresponding equations are provided below [37]:

$$K_{IC} = f\left(\frac{a}{h}\right)\frac{F_{max}S}{Wh^{3/2}} \quad (1)$$

$$f\left(\frac{a}{h}\right) = \frac{3\left(a/H\right)^{1/2}\left[1.99-\left(a/h\right)\left(1-a/h\right)\times\left(2.15-\frac{3.93a}{h}+2.7a^2/h^2\right)\right]}{2\left(1+\frac{2a}{W}\right)\left(1-a/W\right)^{3/2}}$$

where F_{max} is the peak load, S is the span length, W is the specimen thickness, h is the specimen height, a is the notch length, and K_{IC} is the mode I fracture toughness.

Table 3 presents the fracture test results for single-material specimens, including peak load, corresponding displacement, and calculated Mode I fracture toughness. In addition, the corresponding load–displacement curves from fracture tests are shown in Figure 2, allowing direct comparison of the overall fracture response of the two materials. The Mode I fracture toughness values also revealed a clear difference in resistance to crack propagation between the two materials, with Material 1 showing higher toughness. These distinctions provide the necessary mechanical contrast for exploring interfacial fracture behavior in bi-material or composite materials.

3.2. Fracture behavior of bi-material specimens

The fracture behavior of bi-material specimens was examined through three-point bending tests on pre-notched beams. The experimental program involved six configurations, varying in both layer thickness ratio and notch location, as described in Table 1. Each configuration was designed to isolate the effect of either placing the notch in the stiffer material (Material 1) or the weaker material (Material 2), while varying the relative thickness of the layers. In all specimens, a 15 mm edge notch was introduced perpendicular to the interface between the two materials. The aim of this study was not to characterize the interface properties (e.g., bond strength or roughness), but rather to investigate how the mechanical contrast and geometric arrangement of the materials influence the crack growth behavior. To illustrate the fracture response, the load–displacement curves for all six configurations are presented in Figure 3. Each subfigure shows the results for both specimens in a given configuration, allowing direct comparison and evaluation of repeatability.

Overall, the curves demonstrate consistent trends within each configuration, confirming uniform specimen preparation and controlled testing conditions. Notably, dual peak behavior was observed in two configurations (i.e., E-M2 and T2-M2) exhibited a two-stage fracture mechanism: initial fracture propagation within the weaker layer, followed by resistance at the interface and subsequent penetration into the stiffer material. To quantify these observations, Table 4 reports the peak load and displacement at peak for all 12 specimens (two per configuration), along with the average values for each group. A quantitative comparison of the results further highlights the influence of notch location and thickness ratio. With equal layer thickness (E), moving the notch from Material 1 (E-M1, 0.825 kN) to Material 2 (E-M2, 0.780 kN) reduces the peak load by 5.5%. When Material 1 is thicker (T1), specimens notched in Material 2 (T1-M2, 1.300 kN) show an 8.8% higher peak load than those notched in Material 1 (T1-M1, 1.195 kN), highlighting the strong role of geometry when the stiffer layer dominates the section. Conversely, when Material 2 is thicker (T2), placing the notch in Material 2 (T2-M2, 0.530 kN) instead of Material 1 (T2-M1, 0.690 kN) lowers the peak load by 23.2%. For a fixed notch location in Material 1, increasing the thickness of the stiffer layer (E-M1 to T1-M1) raises the peak load by 44.8%, while increasing the thickness of the weaker layer (E-M1 to T2-M1) lowers it by 16.4%. For a fixed notch location in Material 2, making Material 1 thicker (E-M2 to T1-M2) increases the peak load by 66.7%, whereas making Material 2 thicker (E-M2 to T2-M2) decreases it by 32.1%.

For configurations E-M2 and T2-M2, where dual peak behavior was observed, the second peak load and displacement are additionally provided in Table 5. Dual-peak responses (E-M2 and T2-M2) exhibit second peaks lower than the first by 34.6% and 15.1%, respectively (0.51 vs. 0.78 kN; 0.45 vs. 0.53 kN). The displacement at the second peak is approximately 9–11% larger than at the first (0.42 vs. 0.385 mm for E-M2; 0.46 vs. 0.415 mm for T2-M2), consistent with a staged propagation where interfacial processes delay penetration into the stiffer layer and require greater overall deformation.

The experimental results, reflected in both the load-displacement curves (Figure 3) and the quantitative data presented in Tables 4 and 5, reveal consistent trends regarding the influence of notch location and layer thickness on the fracture behavior of bi-material specimens. One clear trend is the effect of notch placement: specimens with notches in the weaker material (Material 2) generally reached lower peak loads compared to those notched in the stiffer material (Material 1), under otherwise identical geometric conditions. In addition, variations in the layer thickness ratio influenced both the load capacity and the deformation characteristics. Increasing the thickness of the weaker material tended to reduce the overall strength and stiffness of the specimens, as reflected in lower peak loads and larger displacements at failure. Conversely, increasing the share of the stiffer material contributed to greater load-bearing capacity.

Another important observation concerns the transition of cracks across the interface, where specimens with notches in Material 1 (the stiffer material) exhibited a sudden load drop after crossing the

Table 3. Results of three-point bending fracture tests on single-material specimens.

Material type	Peak load (kN)	Displacement at peak (mm)	Fracture toughness MPa.m^{05})
Material 1	1.32	0.26	0.46
Material 2	0.44	0.44	0.17

Table 4. Peak load and displacement at peak for bi-material specimens under three-point bending.

Specimen code	Peak load sample 1 (kN)	Peak load sample 2 (kN)	Avg. Peak load (kN)	Displacement sample 1 (mm)	Displacement sample 2 (mm)	Avg. displacement (mm)
E-M1	0.820	0.830	0.825	0.36	0.37	0.37
E-M2	0.780	0.780	0.780	0.41	0.36	0.385
T1-M1	1.190	1.200	1.195	0.33	0.30	0.315
T1-M2	1.290	1.310	1.300	0.30	0.33	0.315
T2-M1	0.670	0.710	0.690	0.43	0.45	0.44
T2-M2	0.540	0.520	0.530	0.43	0.40	0.415

Table 5. Secondary peak load and displacement values for dual-peak specimens.

Specimen code	Second peak load sample 1 (kN)	Second peak load sample2 (kN)	Avg. second peak load (kN)	Displacement sample 1 (mm)	Displacement sample 2 (mm)	Avg. displacement (mm)
E-M2	0.53	0.49	0.51	0.45	0.40	0.42
T2-M2	0.43	0.47	0.45	0.48	0.45	0.46

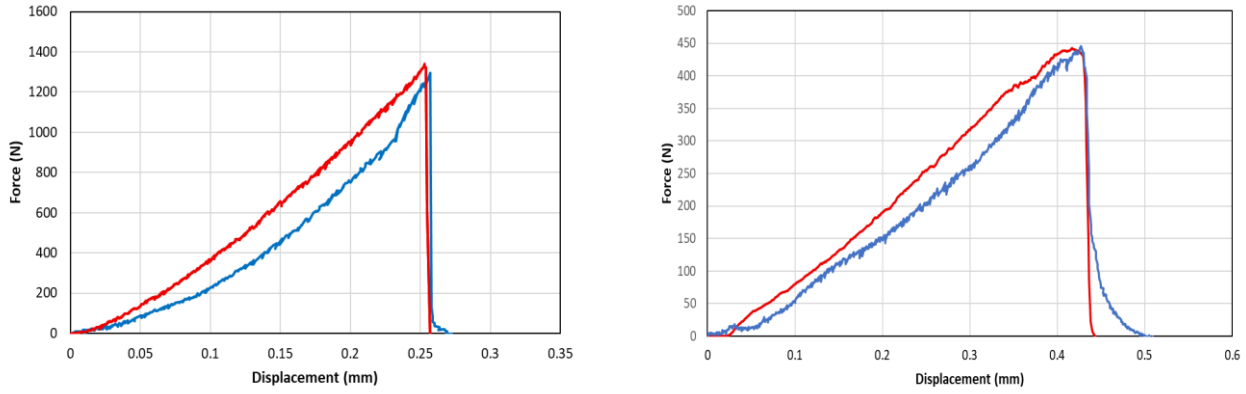

(a) (b)

Figure 2. Load–displacement curves from fracture tests on single-material beams (a) Material 1 (b) Material 2.

interface, whereas those notched in Material 2 (the weaker material) typically showed a smoother transition. In two configurations (i.e., E-M2 and T2-M2) this behavior resulted in dual peak responses, suggesting a two-stage fracture process involving delayed crack progression into the stiffer material due to interfacial resistance.

To complement the quantitative load-displacement analysis, crack trajectories observed in each bi-material configuration are presented in Figure 4. To enhance clarity, the interfaces between the two layers are highlighted with yellow dashed lines.

Figures 4a and 4b present the post-fracture appearances of specimens E-M1 and E-M2, both featuring equal thicknesses of the two materials. In E-M1 (Fig. 4a), where the notch was placed in the stiffer material (Material 1), the crack propagated in a relatively straight path, traversing the interface with no apparent deviation. In contrast, E-M2 (Fig. 4b), with the notch located in the weaker material (Material 2), exhibited a deflected crack path that propagated along the interface before re-entering Material 1. This contrast clearly illustrates the influence of notch location and mechanical mismatch on crack trajectory in bi-material systems. Figures 4c and 4d illustrate the observed crack growth paths for specimens T1-M1 and T1-M2, where Material 1 was the thicker layer. In T1-M1 (Fig. 4c), the notch was located in the thicker and stiffer material, and the crack propagated almost linearly across the interface without any observable deviation, indicating that the stronger layer dominated the fracture path. In contrast, T1-M2 (Fig. 4d), where the notch was in the thinner, weaker layer (Material 2), exhibited deflection along the interface before the crack penetrated into Material 1. This interface deviation contributed to a slightly higher peak load compared to T1-M1, likely due to increased resistance to crack entry. Figures 4e and 4f show the crack propagation paths for specimens T2-M1 and T2-M2, in which Material 2 formed the thicker layer. In T2-M1 (Fig. 4e), the notch was located in the thinner, stiffer material (Material 1). The crack propagated through Material 1 and, upon reaching the interface, continued into the thicker, more compliant Material 2 without deviation. In T2-M2 (Fig. 4f), the crack initiated in the thicker, weaker layer (Material 2) and upon reaching the interface, it temporarily propagated along the interface before penetrating into Material 1. The deflected crack path indicated a staged fracture process influenced by the interface interaction.

4. Conclusion

This study explored the fracture behavior of bi-material rock-like specimens with varying layer thicknesses and notch locations under Mode I three-point bending. Based on the experimental results and

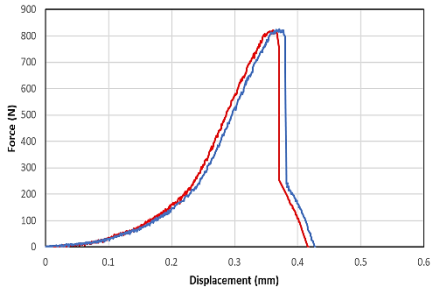

(a). E-M1

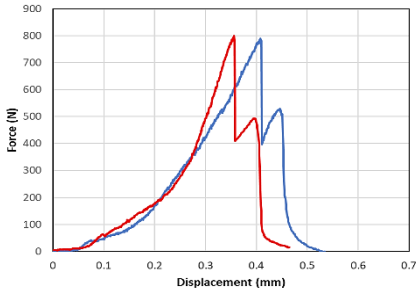

(b). E-M2

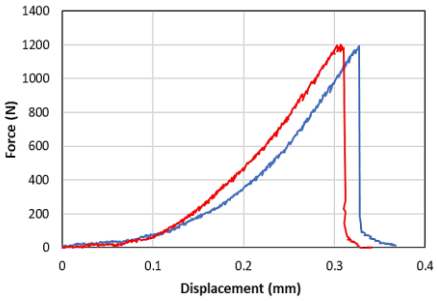

(c) T1-M1

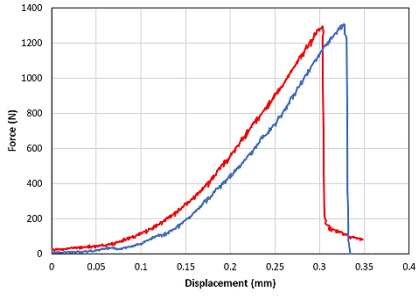

(d) T1-M2

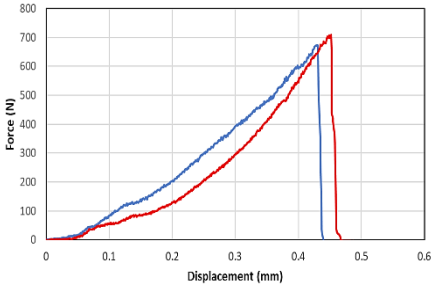

(e). T2-M1

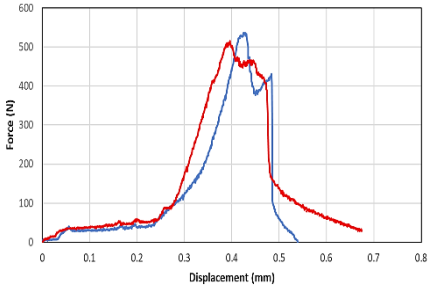

(f). T2-M2

Figure 3. Load–displacement curves of bi-material specimens under three-point bending tests: (a) E-M1, (b) E-M2, (c) T1-M1, (d) T1-M2, (e) T2-M1, (f) T2-M2.

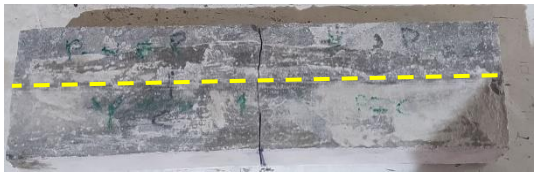

(a). E-M1

(b). E-M2

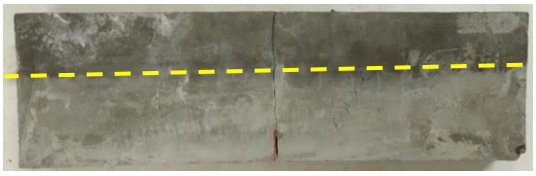

(c). T1-M1

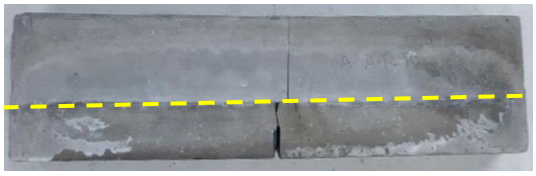

(d). T1-M2

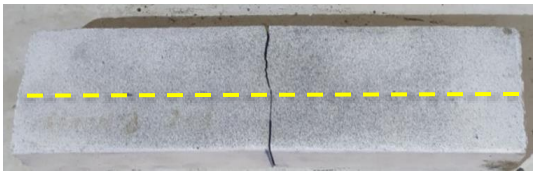

(e). T2-M1

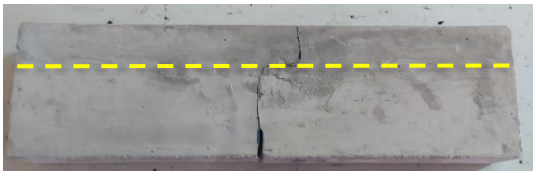

(f). T2-M2

Figure 4. Post-fracture crack trajectories observed in bi-material specimens under three-point bending tests. The yellow dashed line indicates the material interface. (a) E-M1, (b) E-M2, (c) T1-M1, (d) T1-M2, (e) T2-M1, (f) T2-M2.

fracture observations, the following conclusions can be drawn:

- The significant differences in strength and fracture toughness between the two materials resulted in distinct crack behaviors depending on the direction of propagation across the interface.

- Specimens notched in the stiffer material (Material 1) typically exhibited more abrupt failure and higher peak loads, while those with notches in the weaker material (Material 2) showed more gradual crack propagation and, in some cases, staged fracture with interface deflection.

- Increasing the thickness of the stronger material improved load capacity and stiffness, whereas thicker weaker layers were associated with lower peak loads and greater deformations.

- Cracks generally propagated straight across the interface when initiating in the stiffer layer, but tended to deviate along the interface or change direction when initiated in the weaker material.

- These results highlight the importance of considering both material arrangement and interface location in the design of layered or repaired rock structures, especially in cases where directional crack growth may compromise stability.

The outcomes of this research provide a solid experimental basis for understanding crack-interface interactions in quasi-brittle composite systems and can support the calibration and validation of numerical models aimed at simulating fracture in multi-material geomaterials.

While the present study provides valuable insights into crack propagation across bi-material interfaces, certain limitations should be acknowledged. The experiments focused primarily on the effects of notch location and layer thickness, while other influential factors such as interface roughness, bonding quality, and environmental conditions (e.g., moisture, temperature) were not explicitly investigated. These aspects are known to play a role in controlling fracture initiation and propagation and may alter the observed mechanisms. Future studies incorporating these interfacial characteristics, as well as numerical simulations, would provide a more comprehensive understanding of fracture behavior in layered rock-like materials.

References

[1]. Chen J, Zhou L, Zhang X, Zhuang J, Liu Z (2025) Study on the mechanisms of tensile failure in rock-shotcrete interfaces induced by stress waves. Engineering Fracture Mechanics:111193

[2]. Chen J, Zhou L, Zhu Z, Ma L, Shui X, Wang M (2024) The influence of interface morphology on the tensile properties and interface stress of rock-shotcrete Brazilian discs. Case Studies in Construction Materials 20:e03029

[3]. Wang W, Su H, Zhao H, Yu L, Wu C (2023) Experimental investigation on mode I fracture behavior of sandstone after grouting filling under three-point bending. Engineering Fracture Mechanics 291:109578

[4]. Wang H-W, Wu Z-M, Wang Y-J, Yu RC (2020) Investigation on crack propagation perpendicular to mortar–rock interface: Experimental and numerical. International Journal of Fracture 226:45-69

[5]. Cook T, Erdogan F (1972) Stresses in bonded materials with a crack perpendicular to the interface. International Journal of Engineering Science 10:677-697

[6]. Kaddouri K, Belhouari M, Bouiadjra BB, Serier B (2006) Finite element analysis of crack perpendicular to bi-material interface: Case of couple ceramic–metal. Computational materials science 35:53-60

[7]. Silling SA, Askari E (2005) A meshfree method based on the peridynamic model of solid mechanics. Computers & structures 83:1526-1535

[8]. Askari E, Xu J, Silling S (2006) Peridynamic analysis of damage and failure in composites. In: 44th AIAA aerospace sciences meeting and exhibit, p 88

[9]. Xu J, Askari A, Weckner O, Razi H, Silling S (2007) Damage and failure analysis of composite laminates under biaxial loads. In: 48th AIAA/ASME/ASCE/AHS/ASC structures, structural dynamics, and materials conference, p 2315

[10]. Zak A, Williams ML (1963) Crack point stress singularities at a bi-material interface.

[11]. Ha YD, Bobaru F (2011) Dynamic brittle fracture captured with peridynamics. In: ASME International Mechanical Engineering Congress and Exposition, pp 437-442

[12]. Kefayati S, Eftekhari M, Goshtasbi K, Ahmadi M (2025) Evaluating shear strength and acoustic emission in rock-like materials with non-persistent joint geometries under freeze-thaw conditions. Scientific Reports 15:20488

[13]. Kefayati S, Ahmadi M, Goshtasbi K, Eftekhari M (2025) Effect of Non-persistent Joint Distribution on Crack Growth and Shear Behavior in Andesite Using a Lattice-Spring Synthetic Rock Mass Approach. Geotechnical and Geological Engineering 43:69

[14]. Doostan A, Eftekhari SM, Ahmadi M (2024) Experimental Investigation of the Effect of Grain Size on the Mechanical Parameters and Mode I Fracture Toughness of Rock-Like Materials. JOURNAL OF ROCK MECHANICS 8:21-34

[15]. Hillerborg A, Modéer M, Petersson P-E (1976) Analysis of crack formation and crack growth in concrete by means of fracture mechanics and finite elements. Cement and concrete research 6:773-781

[16]. Zhang J, Wang Z, Ju X, Shi Z (2014) Simulation of flexural performance of layered ECC-concrete composite beam with fracture mechanics model. Engineering Fracture Mechanics 131:419-438

[17]. Wäppling D, Gunnars J, Stahle P (1998) Crack growth across a strength mismatched bimaterial interface. International Journal of Fracture 89:223-243

[18]. Freed Y, Banks-Sills L (2008) A new cohesive zone model for mixed mode interface fracture in bimaterials. Engineering Fracture Mechanics 75:4583-4593

[19]. Dong W, Wu Z, Zhou X, Dong L, Kastiukas G (2017) FPZ evolution of mixed mode fracture in concrete: Experimental and numerical. Engineering Failure Analysis 75:54-70

[20]. Dong W, Yang D, Zhang B, Wu Z (2018) Rock-concrete interfacial crack propagation under mixed mode I-II fracture. Journal of Engineering Mechanics 144:04018039

[21]. Buyukozturk O, Hearing B (1998) Crack propagation in concrete composites influenced by interface fracture parameters. International Journal of Solids and Structures 35:4055-4066

[22]. Zhou M, Zhang W, Xu Y, He F, Wang Y, Dong S (2024) Influence of substrate properties on fracture behavior of rock-concrete bi-material central interface cracked Brazilian disks at different loading angles. Theoretical and Applied Fracture Mechanics 134:104757

[23]. Wu D, Su H, Yu L, Zhang F, Qin H, Wei C, Geng S (2024) Experimental and numerical investigation of dynamic tensile behavior of granite-concrete bimaterials with different rough interfaces. Journal of Building Engineering 84:108565

[24]. Liu J, Zeng X, Zheng W, Lai H, Wang Y, Wang F, Qiu H (2025) Dynamic behavior of a running crack crossing mortar-granite interface with different interface inclinations. Engineering

Fracture Mechanics 314:110705

[25]. Miao Z, Li S, Liang Y, Huo R, Qi H, Yin X, Yu Z (2025) Macro and micro damage and degradation mechanism of granite-concrete interface under acidic dry-wet cycles. Journal of Building Engineering 104:112332

[26]. Liu S, Zhao J, Cheng F, Yu H, Chen J (2024) Mechanical Behavior and Failure Mechanism of Rock–Concrete Composites Under the Coupling Effect of Inclined Interface Angle and Ground Temperature. Symmetry 17:52

[27]. Colavito K, Kilic B, Celik E, Madenci E, Askari E, Silling S (2007) Effect of nanoparticles on stiffness and impact strength of composites. In: 48th AIAA/ASME/ASCE/AHS/ASC structures, structural dynamics, and materials conference, p 2021

[28]. Zhou X-P, Wang Y-T (2016) Numerical simulation of crack propagation and coalescence in pre-cracked rock-like Brazilian disks using the non-ordinary state-based peridynamics. International Journal of Rock Mechanics and Mining Sciences 89:235-249

[29]. Eftekhari M, Xu C (2023) Evaluating MTS criterion in predicting mixed - mode crack extension under different loading conditions. Fatigue & Fracture of Engineering Materials & Structures 46:96-110

[30]. Afrasiabian B, Eftekhari M (2022) Prediction of mode I fracture toughness of rock using linear multiple regression and gene expression programming. Journal of Rock Mechanics and Geotechnical Engineering 14:1421-1432

[31]. Eftekhari M, Baghbanan A, Mohtarami E, Hashemolhosseini H (2017) Determination of crack initiation and propagation in two disc shaped specimens using the improved maximum tangential stress criterion. Journal of Theoretical and Applied Mechanics 55:469-480

[32]. Eftekhari M, Baghbanan A, Hashemolhosseini H (2016) Crack propagation in rock specimen under compressive loading using extended finite element method. Arabian Journal of Geosciences 9:145

[33]. Eftekhari M, Baghbanan A, Hashemolhosseini H, Amrollahi H (2015) Mechanism of fracture in macro-and micro-scales in hollow centre cracked disc specimen. Journal of Central South University 22:4426-4433

[34]. Eftekhari M, Baghbanan A, Hashemolhosseini H (2015) Extended finite element simulation of crack propagation in cracked Brazilian disc. Journal of Mining and Environment 6:95-102

[35]. Eftekhari M, Baghbanan A, Hashemolhosseini H (2015) Fracture propagation in a cracked semicircular bend specimen under mixed mode loading using extended finite element method. Arabian Journal of Geosciences 8:9635-9646

[36]. Eftekhari M, Baghbanan A, Hashemolhosseini H (2014) Determining stress intensity factor for cracked Brazilian disc using extended finite element method. International Journal of Scientific Engineering and Technology 3:890-893

[37]. Huang Y, Guan Y, Wang L, Zhou J, Ge Z, Hou Y (2018) Characterization of mortar fracture based on three point bending test and XFEM. International Journal of Pavement Research and Technology 11:339-344Porter K. A beginner's guide to fragility, vulnerability, and risk. University of Colorado Boulder, 119 pp 2019.